Food Chemistry: X 24 (2024) 101853

Contents lists available at ScienceDirect

Food Chemistry: X

journal homepage: www.sciencedirect.com/journal/food-chemistry-x

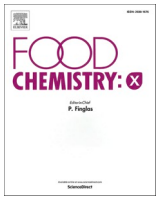

Effect and mechanism of green and aldehyde aroma compounds from sweet orange on sucrose sweetness perception

ZuoBing Xiao [a,b,d], HouWang Wang [a], YunWei Niu [a], JianCai Zhu [a], Yamin Yu [a], YuanBin She [c], RuJun Zhou [a], Zhaogai Wang [d], Jing Zhang [a,*]

[a] School of Perfume and Aroma Technology, Shanghai Institute of Technology, Shanghai 201418, China
[b] School of Agriculture and Biology, Shanghai Jiao Tong University, Shanghai 200240, China
[c] College of Chemical Engineering, Zhejiang University of Technology, Hangzhou 310014, China
[d] Agricultural Products Processing Center, Henan Academy of Agricultural Sciences, Zhengzhou 450008, China

ARTICLE INFO

Keywords:
Green aroma
Aldehyde aroma
Aroma and taste
Electronic tongue
Molecular simulation

ABSTRACT

At present, there are relatively few studies on the influence of green aroma and aldehyde aroma compounds on the sweetness perception of sucrose. This study examined the effects of 11 aroma compounds from sweet orange, characterized by green and aldehyde flavors, on the sweetness of a 5 % sucrose solution. Using artificial sensory analysis and electronic tongue technology, it was found that most aromatic compounds can inhibit sweetness perception, and the inhibitory effect of trans-2-decenoaldehyde is the most significant. The mechanism of inhibition was explored through molecular simulation, revealing that the binding free energy of molecular docking was greater than −5.9 kcal/mol. Further molecular dynamics analysis showed that compared with the T1R2/T1R3 sucrose binary system, the addition of aroma substances reduced the number of hotspot residues involved in protein ligand binding, and did not enhance the binding ability of ligand proteins, indicating an inhibitory effect.

1. Introduction

Citrus resources boast abundance, comprising a plethora of excellent varieties. Among these, sweet orange stands as a beloved choice among the public, esteemed for its distinctive flavor profile and rich array of nutrients. The fragrance of sweet orange encompasses a spectrum of notes, including sweet, fruity, floral, green, and aldehydes (Xiao et al., 2023). Previous research has underscored the pivotal role of green and aldehyde aromas in shaping the characteristic aroma of sweet orange (Pan et al., 2023), with compounds such as α-pinene, decanal, and β-pinene emerging as significant contributors to the aroma profile of orange juice (Perez-Cacho & Rouseff, 2008). While citrus and fruit aromas constitute the primary aroma components in sweet orange juice, green and aldehyde notes, albeit minor, play an indispensable role. They exert a modulatory influence on the overall aroma of orange juice, enhancing its depth and complexity (Shui et al., 2019).

The escalating health concerns due to high-sugar diets have captured increasing consumer attention. To address the dual demands of food safety and flavor, the pursuit of "reducing sugar without reducing sweetness" has emerged as a pivotal research focus within the food industry (Alcaire et al., 2017). Odor-induced taste enhancement (OITE) presents a promising avenue that not only caters to the "low sugar" trend but also upholds food flavor quality, offering a novel approach to sugar reduction and sweetness augmentation. OITE operates on the principle of "Cross-modal sensory compensation," wherein stimuli from one sensory modality can bolster the satisfaction associated with another sensory modality (Biswas & Szocs, 2019). By leveraging specific odors, taste perception intensity is amplified (Ai & Han, 2022). Previous investigations have identified aromas with sweet attributes—such as floral, fruity, and sweet scents—as capable of heightening human perception of food sweetness (Aveline et al., 2023; Boakes & Hemberger, 2012). For instance, Xiao et al. (2021) identified eight odors in bananas, including 3-methylbutyl acetate, 2-methylpropyl acetate, pentyl acetate, and 3-methylbutyl butanoate, which significantly enhanced the sweetness of a 30 g/L sucrose solution. Similarly, Romeo-Arroyo et al. (2022) demonstrated that vanilla aroma could augment sweetness perception in butter cookies.

The modulation of sweetness perception by volatile flavor

* Corresponding author at School of Perfume and Aroma Technology, Shanghai Institute of Technology, Shanghai 201418, China.
E-mail addresses: sitflavor@163.com (Z. Xiao), wongxx5556@163.com (H. Wang), nyw@sit.edu.cn (Y. Niu), zjc01@163.com (J. Zhu), yuyamin@sit.edu.cn (Y. Yu), sheyb@zjut.edu.cn (Y. She), zhourj@sit.edu.cn (R. Zhou), zgwang1999@126.com (Z. Wang), zhangj@sit.edu.cn (J. Zhang).

https://doi.org/10.1016/j.fochx.2024.101853
Received 4 August 2024; Received in revised form 18 September 2024; Accepted 20 September 2024
Available online 23 September 2024

compounds involves a complex interaction between olfactory and taste receptors, leading to an enhanced neural response to specific odors, which in turn influences the perception of sweetness. The sense of olfaction occurs through two distinct pathways: orthonasal and retronasal (Small et al., 2005). Orthonasal olfaction refers to the perception of smells that enter the nasal cavity directly through inhalation, while retronasal olfaction occurs when odorant compounds released during food processing (e.g., chewing and swallowing) travel to the olfactory epithelium via the oropharyngeal pathway. These compounds bind to olfactory receptors, triggering olfactory perception (Small et al., 2005). Kakutani et al. (2017) simulated the olfactory transmission system through both the nasal and retronasal pathways by delivering odor stimuli simultaneously to the nasal and oral cavity via separate tubes. Despite identical odor intensity from both routes, the study found that sweetness enhancement of sucrose solution was only significant through the retronasal pathway, not the orthonasal route. Post-nasal odors have long been associated with oral perception, and odorants dissolved in sweetener solutions may stimulate both taste receptors in the mouth and olfactory receptors in the nasal cavity. Consequently, post-nasal odors are often attributed to taste perception (Han & Hummel, 2019).

Although current research on how different aroma characteristics affect the perception of sweetness in sweet substances is advancing, it is still relatively superficial. It mainly focuses on the influences of sweet and fruity aroma compounds, while the interactions between green and aldehyde aromas and sweetness have been less explored. Furthermore, most existing studies on Odor-Induced Taste Enhancement (OITE) predominantly rely on subjective artificial sensory evaluation methods, lacking substantive evidence from objective instrumental analysis techniques.

The perception of taste in individuals relies on taste receptor proteins, which, upon interaction with flavor components, transmit signals to the body, eliciting taste responses (Precone et al., 2019). Sweet receptors T1R2/T1R3 belong to the C subtype of GPCRs, the first family of taste receptors, which exist in the form of heterodimers (Strazzullo et al., 2009). The structure of T1R2/T1R3 comprises extracellular domains, namely the Amino Terminal Domain (ATD) and Transmembrane Domain (TMD), with the ATD further subdivided into the Venus Flytrap Domain (VFD) and Cysteine-rich Domain (CRD) (Rother et al., 2018). As the N-terminal domain, the VFD harbors active sites crucial for interacting with various sweeteners, posited as the primary binding site for sweeteners to receptor proteins. Olfactory receptors (ORs) are proteins that detect odor molecules. These chemosensory receptors, found in the olfactory organs of animals, bind to specific odorants (Malnic et al., 2004). Classified as G protein-coupled receptors (GPCRs), they feature seven transmembrane helical domains. The human genome includes a substantial number of olfactory receptor genes, which constitute approximately 50 % of the GPCR family. These genes are extensively but unevenly distributed across chromosomes (Vadevoo et al., 2021). In this study, we focused on two specific olfactory receptors: OR1A1 and OR52D1. OR1A1 is characterized as a broadly tuned receptor, responding to a diverse array of molecular structures that serve as agonists (Ahmed et al., 2018). Likewise, OR52D1 is known for its broad responsiveness, enabling it to detect a variety of aromatic compounds (Tong et al., 2021). However, studying sweet receptor proteins in vitro is challenging due to difficulties in protein purification and culturing, often resulting from low protein concentrations. As a result, employing molecular simulation to forecast the binding process between receptor proteins and ligands stands as an effective strategy for elucidating the mechanisms governing flavor substances' taste presentation at the molecular level (Tao et al., 2020).

Yousif et al. (2020) employed homology modeling to predict the complete 3D structure of the T1R2/T1R3 receptor. Acevedo et al. (2018) utilized molecular docking to study the interaction of six monosaccharides (glucose, galactose, fructose, xylose, sucrose, and tagatose), three artificial sweeteners (sucralose, saccharin, and aspartame), and several natural sweeteners (various isomers of monatin, glycyrrhizin, mogroside V, active compounds of stevia, and several sweet proteins) with the T1R2/T1R3 receptor. Their findings revealed a negative correlation between the binding affinity and sweetness intensity; a lower binding energy indicated a higher perceived sweetness. Miao et al. (2022) conducted a molecular docking analysis of 28 sweeteners across four categories: natural sugars, natural sugar alcohols, artificial amides, and artificial dipeptide derivatives. They found that the strength of interaction between the sweeteners and the receptor could account for differences in sweetness perception. Hydrophilic sugars and sugar alcohols interacted with the receptor primarily through numerous hydrogen bonds, yet they exhibited weaker sweetness intensity. Furthermore, mechanical simulations of eight typical sweeteners binding to the T1R2-membrane system revealed that hydrophobic forces significantly contributed to the binding of artificial high-intensity sweeteners. As sweetness intensity perception decreased, sweeteners demonstrated three binding states: close binding to the VFT domain, a tendency to release, and full release. Additionally, it was suggested that potent sweeteners might act as inhibitors by overstimulating the T1R2/T1R3 receptors, hindering their timely release. Malnic et al. (1999) utilized molecular docking technology to investigate the key volatile compounds in coffee leaves. Their research identified pentanal and methyl salicylate as potential activators of the olfactory receptors OR5M3 and OR1G1, respectively. These compounds are believed to be responsible for the characteristic fresh and fragrant notes of coffee leaves. However, there are few current reports on the interactions within ternary systems that involve two ligands—odor and taste substances—and receptor proteins, particularly regarding the interplay between aroma and taste.

In this study, we investigated the effects of 11 green and aldehyde aroma compounds found in sweet orange on sweetness perception. The research included several key steps: analyzing the threshold values of various green and aldehyde aroma compounds in a sucrose solution; assessing the impact of these 11 aroma compounds on the sweetness and palatability of a 5 % sucrose solution using a combination of artificial sensory analysis and electronic tongue bionic technology; employing molecular docking to summarize the effects of aroma addition on the binding parameters of sucrose with sweet receptors, and to explore the interaction mechanism through changes in binding sites and energies within the T1R2/T1R3-aroma-sucrose ternary system; investigating the impact of aromatic compounds on two olfactory receptors, OR1A1 and OR52D1, and their subsequent influence on taste perception intensity; conducting molecular dynamics simulations of the T1R2/T1R3-aroma-sucrose ternary system to explore the dynamic interaction processes. This study enhances our understanding of how different aroma characteristics of volatile substances influence the sweetness perception of sweet compounds and their mechanisms of action. The findings offer valuable insights for the development and application of fruit flavors and other related products.

2. Materials and method

2.1. Experimental materials

In this study, we investigated the key green and aldehyde aromatic compounds found in sweet orange, including α-pinene, β-pinene, 3-carene, terpinen-4-ol, 1-decanol, trans-2-decenal, α-terpineol, tetradecanal, dodecanol, decanal and sabinene. These compounds were sourced from Shanghai Meixin Chemical Technology (China). Edible grade sucrose was purchased from Henan Wanbang Industrial (China). Distilled water purchased from A.S. Waston Trademarks Limited (A.S.WATSON TM LIMITED). All experimental materials were of edible grade, ensuring the safety and reliability of our experiments. The experiment was conducted in a safe and ventilated laboratory, with the selected concentration of aroma substances within a safe range.

2.2. The aroma threshold in sucrose solution was determined by the S-curve

According to previous literature reports (Bertelsen et al., 2020; Cometto-Muñiz & Abraham, 2016), the logarithmic concentration and detection probability of each pure compound follow an S-curve ($p = 1$ (1 + $e^{-(x-t)/D}$), P is the detection probability, x is the logarithmic concentration of the aroma compounds, t is the threshold of the aroma, and D is the steepness of the function). Due to the varying maximum recommended dosages for each aroma, different concentration gradients must be established to detect the threshold values of various green and aldehyde compounds in sucrose. The threshold determination experiment should be determined by three-point selection method (3-AFC) method: 11 green and aldehyde aroma compounds are dissolved in a sucrose solution, and the maximum concentration of each aroma is adjusted based on the estimated threshold value or the threshold concentration in water reported in the literature. Serial dilutions are then performed from the highest concentration downward. To uniformly disperse non-polar aroma compounds in the sucrose solution, propylene glycol was used as a co-solvent, utilizing an ultrasonic device to facilitate dispersion. Propylene glycol is a colorless, nearly tasteless liquid with a slightly sweet smell, and its threshold in water is 340 mg/L (Gemert, L. v. 2003). We first dissolved the aroma compounds in propylene glycol, then diluted the mixture to a specific concentration before adding it to a 5 % sucrose solution. The detection thresholds for green and aldehydes are generally lower than that of propylene glycol. Therefore, given the lower thresholds of the aroma compounds, the sweetening effect of propylene glycol is considered negligible. If participants can correctly identify the sucrose solution containing the aromatic compound, the same test is conducted at the next lower concentration, with sequential dilutions continuing. The responses of the participants are recorded, and the detection probability (P) is calculated as the ratio of correct responses to the total number of participants. The corrected detection probability is determined using the correction formula $P^* = (3P - 1) / 2$, where P* represents the corrected detection probability and P is the actual detection probability. Finally, the curve is drawn by Origin software, and the corresponding horizontal coordinate is defined as the threshold value when the vertical coordinate $P = 0.5$.

2.3. Sweetness influence analysis

2.3.1. Artificial sensory evaluation

Following methods from previous studies (Dai et al., 2018; Miyazawa et al., 2009), the evaluation team comprised 10 reviewers (4 males and 6 females, aged 22–32), all of whom were healthy, free of bad habits, and had extensive experience in sensory analysis. The team members are students from the Shanghai Institute of Technology. None of the participants exhibited sensory deficits and all demonstrated the ability to correctly identify the five basic tastes: sour, sweet, bitter, salty, and umami. Participants provided informed consent via the statement “I am aware that my responses are confidential, and I agree to participate in this sensory evaluation” where an affirmative reply was required to enter the sensory evaluation. They were able to withdraw from the sensory evaluation at any time without giving a reason. The “human sensory ethical inspection” was provided in the supplementary material (Fig. S1). The application was submitted to the Human Ethics Committee of the school. With the approval of the committee, the experiment plan was feasible and controllable, and the sensory group participated in the experiment voluntarily.

Five concentration gradients were established based on the actual threshold values measured using the S-curve method, as well as the recommended dosages (Guo et al., 2018; Xiao et al., 2023; Zhou & Xiao, 2007). Each aroma-active compound was tested at both a high and low concentration. The high concentration did not exceed the recommended level to ensure safety, while the low concentration was kept above the threshold to ensure that the detectable concentration in sweet orange remained within the gradient (Table S2). To ensure the reliability of the sensory assessment, group members were instructed to avoid consuming spicy food, using strongly scented personal care products, smoking, or eating for one hour before the test. In this study, participants evaluated two attributes: sweetness and comfort. A 10-point scale was used for both attributes, with sweetness rated from 1 (no sweetness) to 10 (extremely sweet), and comfort rated from 1 (extremely poor comfort) to 10 (extremely good comfort). Comfort level indicates the acceptability of the test solution by team members. Evaluation results were recorded to one decimal place. In the control group, the fixed values for the sweetness and comfort of a 5 % sucrose solution were set at 5. To maintain anonymity and reliability, samples were presented to participants in randomized orders. Experimental samples were prepared within 12 h before the experiment and stored at 8 °C until use. The experiments were conducted in a fume hood at room temperature.

2.3.2. Electronic tongue

The electronic tongue, as a rapid detection tool for food flavor, overcomes the limitations of traditional sensory evaluation, such as high time consumption and subjectivity, by providing an objective assessment of food flavor (Ciursa & Oroian, 2021). In this experiment, we used the Insent TS-5000Z electronic tongue, which is equipped with various sensors capable of detecting tastes like sour, sweet, bitter, salty, and umami. These taste sensors respond to the test sample by converting the response value into an electrical signal. The signal is then processed by a pattern recognition system, which outputs the corresponding taste result (Oroian et al., 2018). For this study, the response value from the sweetness sensor was used as the monitoring index to investigate the impact of different concentrations of green and aldehyde aroma compounds on the sweetness value of a 5 % sucrose solution. Before testing, the electronic tongue's stability was confirmed through a self-test, and sample analysis was conducted only after a successful self-test. A series of detection solutions with varying concentration gradients were prepared to observe sweetness changes for each sample. Each sample was tested in parallel six times, and the average of the measured data was recorded as the sample's sweetness value.

2.4. Molecular simulation

2.4.1. Molecular docking

Molecular docking analysis was conducted using AutoDock Vina software to investigate the interactions of 11 green and aldehyde compounds with the T1R2/T1R3 sweet taste receptor system and with olfactory receptors OR1A1 and OR52D1. The 3D structure of human sweet taste receptor T1R2/T1R3 was self-constructed by our research group according to homologous modeling method. The protein structures of human olfactory receptors OR1A1 and OR52D1 were predicted by AlphaFold. The SDF format file of each small molecule substance was obtained from Pubchem database and converted from SDF format to PDB format through Openbabel software for pre-experimental processing for subsequent molecular docking.

Molecular docking experiments were performed using AutoDockTools (ADT) V1.5.6 and AutoDock Vina V1.2.0 (https://vina.scripps.edu/). The semi-flexible method is adopted for docking (Roy et al., 2018), Prediction of active pockets of protein models by DeepSite. The active center coordinates of VFD structure cavity of T1R2 are (17.9, −20.0, −16.6) (Jiménez et al., 2017); the binding site coordinates of OR1A1 receptor proteins are (12.1, 9.2, −13.3), located in the intracellular TM5 region ; for OR52D1 receptor proteins, the binding site coordinates are (−17.6, −10.5, 12.3), located in the intracellular TM6 region. Using AutoDock Vina to establish a docking model of T1R2/T1R3-aroma, and then docking sucrose with it to form a new ternary system docking model. The docking data were analyzed and the best conformation was selected to explore the change of sweetness value under the ternary system. The 3D structure model of the binding site was drawn by the 3D visualization software Pymol (Yuan et al., 2017), and

the two-dimensional interaction map of protein-ligand was generated by LigPlot+ (Agrawal et al., 2023).

2.4.2. Molecular dynamics simulation

In order to further optimize the binding mode of the complex-protein complex, molecular dynamics simulations were performed using the Desmond procedure. The OPLS4 force field is used for the parameterization of proteins and small molecules, and the SPCE model is used for the water solution. The protein-small molecule ligand complex was placed in a cubic water tank and solvated. The charge in the system was neutralized by adding 0.15.M chlorine examples and sodium ions. Initially, the steepest descent minimization method of 50,000 steps was used to minimize the energy of the system, and secondly, the position of the heavy atoms was restricted to 50,000 steps for NVT and NPT equilibrium. The system temperature is maintained at 300 K and the system pressure is guaranteed at 1 bar. After the two equilibrium stages are completed, 100 ns simulation is performed. The Maestro 2023 was used to analyze the experimental results and generate dynamic trajectories.

2.5. Statistical analysis

SPSS statistical software (IBM, version23) was used for significance analysis, and one-way analysis of variance (ANOVA) was used for artificial sensory sweetness value to analyze the score data of each sensory person on sensory attributes, and Duncan's multiple comparison analysis was combined to determine whether there was any difference from 0. The statistical significance level is 5 % ($p < 0.05$). Origin 2021 software is used for data analysis and plotting.

3. Results and discussion

3.1. Determination of the thresholds of green and aldehyde

Initially, the thresholds of 11 kinds of green and aldehyde compounds in a 5 % sucrose solution were measured by S-curve method and compared with their reference thresholds in water. Table 1 presents the threshold values in the sucrose solution, the reference thresholds in water (Gemert, 2003), and the aroma descriptions of the 11 compounds. Compared with the threshold in pure water system, the measured threshold of α-terpineol in a 5 % sucrose solution decreased by three times, indicating that its unique green and violet aromas are more pronounced in the sucrose solution. In contrast, the thresholds of α-pinene, β-pinene, 3-carene, terpinen-4-ol, trans-2-decenal, dodecanol, and decanal were significantly higher than those in water, suggesting that their green, aldehyde, and lipid odors were generally masked in the sucrose solution. This indicates that interactions with sucrose molecules might weaken the volatility of these substances. There was no significant difference between the measured thresholds of 1-decanol and sabinene and those in pure water. (See Fig. 1.)

The reduction in the volatility of aroma substances in a sucrose solution can be analyzed from two perspectives: physicochemical properties and molecular interactions. From the perspective of changes in

Table 1
Threshold value, reference value and flavor description of 11 green and aldehyde in 5 % sucrose solution.

NO	Aroma	3D Conformer	Threshold (sucrose) mg/Kg	Reference threshold(water)mg/kg	VS (water: sucrose)	Flavor description
1	α-pinene	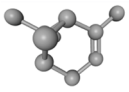	0.90625	0.041	0.045241	Pine，citrus peel，woody
2	β-pinene	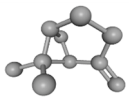	1.28125	0.14	0.109268	Wood，terpene-like，pungent
3	3-carene	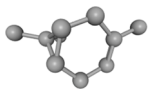	12.03	0.77	0.064007	Pine-like
4	terpinen-4-ol	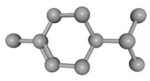	3.90625	1.2	0.3072	Woody，floral
5	1-decanol	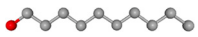	1.7361	0.775	0.446403	Orange blossom、Oil odor
6	trans-2-decenal	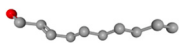	0.0625	0.0004	0.0064	Aldehyde
7	α-terpineol	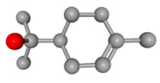	3.0625	9.18	2.997551	Green，violet
8	tetradecanal	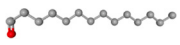	4.1625	0.0021	0.000505	Fatty、Wax
9	dodecanol	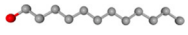	3.1625	0.016	0.005059	violet、Oil odor
10	decanal	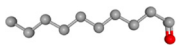	0.13	0.003	0.023077	Green，citrus-like
11	sabinene	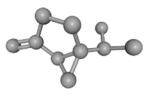	0.95	0.98	1.031579	Earthy

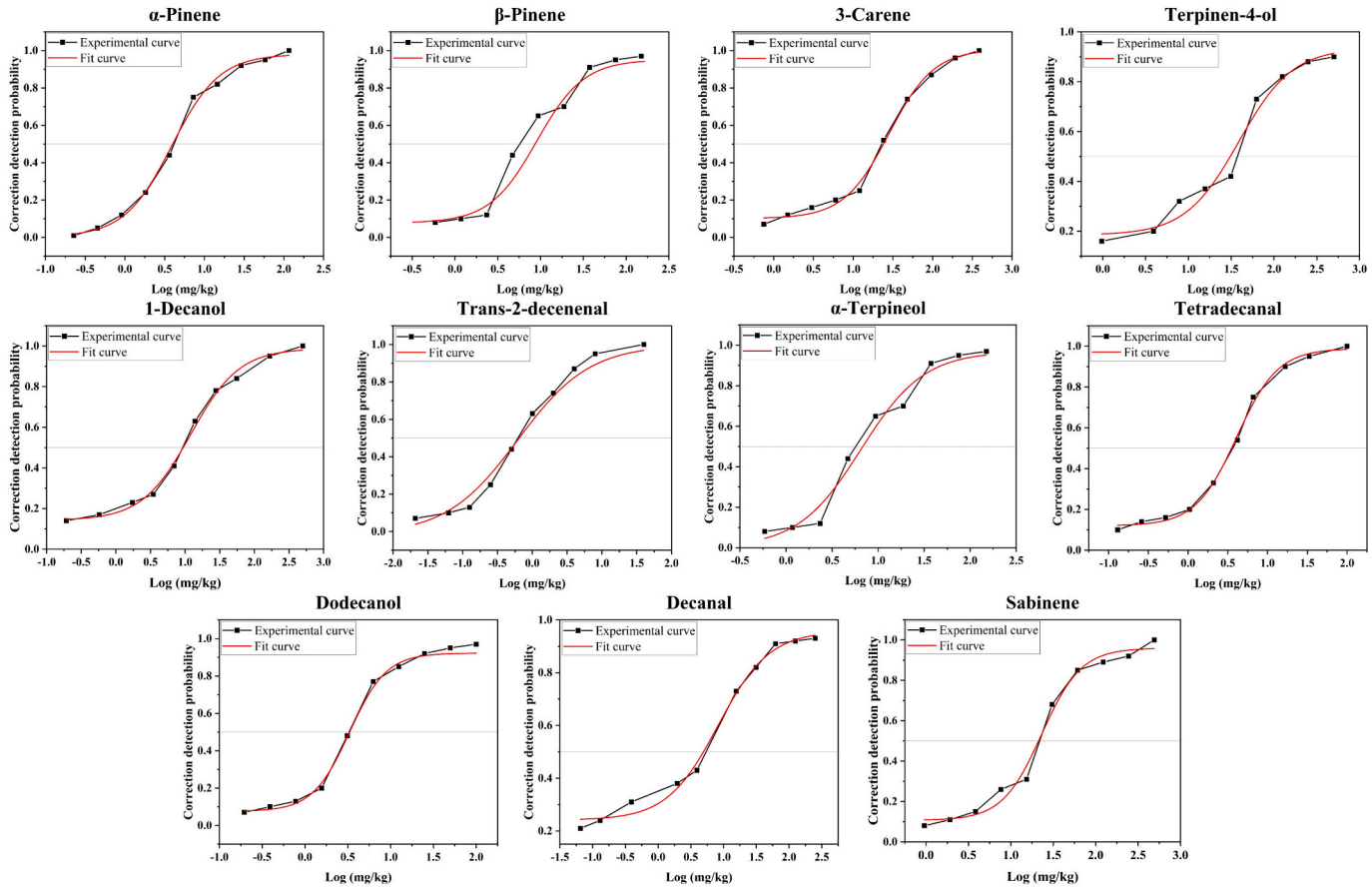

Fig. 1. Threshold value of 11 kinds of green and aldehyde in 5 % sucrose solution. (For interpretation of the references to colour in this figure legend, the reader is referred to the web version of this article.)

physicochemical properties, first of all, compared to pure water, the increase in solute concentration in a sucrose system leads to an increase in solution density. Sucrose, being a polar molecule, may form stable solvation layers around aroma substances such as Trans-2-decenal, thereby reducing their volatility. Additionally, research has established a relationship between the aroma threshold and the carbon chain length of compounds like alcohols and aldehydes. Abraham et al. (2001) demonstrated that the aroma threshold of these compounds generally decreases with an increase in carbon atom count. Cometto-Muñiz and Abraham (2008) further explored this trend for four groups of alcohols (ethanol, n-butanol, n-hexanol, n-octanol) and found that as the carbon chain lengthened, the detection threshold shifted to lower concentrations. Additionally, from the perspective of molecular interactions, aroma compounds may form numerous hydrogen bonds and van der Waals forces with sucrose molecules, leading to closer associations and reduced volatility of aldehydes and alcohols. These interactions can effectively weaken the aroma's volatility.

3.2. *Influence of aroma on sweetness of sucrose*

3.2.1. *Artificial sensory evaluation*

Previous research has indicated that odor-induced taste enhancement is more significant in solutions with low to moderate taste concentrations, and becomes weaker or even undetectable at high concentrations (Xiao et al., 2021). Accordingly, this study selected a 5 % sucrose solution, which has a medium-low sweetness value, as the control group. We then investigated how green and aldehyde compounds affect the sweetness perception of this sucrose solution. The results revealed significant differences in how these 11 compounds affected sweetness perception. Notably, β-pinene, tetradecanal, and dodecanol has significant sweetening effects at certain concentrations ($p < 0.05$). As depicted in Fig. 2, the sweetness values of β-pinene and tetradecanal increased with concentration. However, the woody aroma of β-pinene reduced comfort as its concentration rose, while the fatty and waxy aroma of tetradecanal did not impact sweetness comfort. Dodecanol's sweetness value rose at low concentrations but fell at high concentrations, possibly because its oily aroma became more pronounced and lessened sweetness perception. On the other hand, trans-2-decenal, α-terpineol, and terpinen-4-ol inhibited sweetness perception at certain concentrations. *Trans*-2-Decenal (1 mg/kg-40 mg/kg) demonstrated a relatively pronounced inhibitory effect at low concentrations, with its distinctive aldehyde and sharp pungent odor producing unpleasant perceptions. α-terpineol (30 mg/kg-60 mg/kg) and terpinen-4-ol (8 mg/kg-32 mg/kg) showed more significant inhibitory effects with increasing concentration at higher concentrations, which may be due to the inconsistency between the aroma of pepper, convallaria and sweet smell. Previous studies have also shown that not all sweeteners enhance sweetness perception (Barba et al., 2018). For instance, ethyl 2-methylbutanoate, furaneol, and gamma-decalactone were found to significantly improve the sweetness of a 7 % sucrose solution, while others did not. Xiao et al. (2021) found that ethyl acetate as “fruity and sweet” during GC-O olfactory process but did not significantly enhance sweetness, possibly because participants believed that ethyl acetate was an organic solvent with low acceptability, leading to unpleasant perceptions. In general, the sweetness perception brought by green and aldehyde compounds is not significant at low concentrations, and some compounds may even inhibit sweetness at high concentrations. The intensity of unpleasant odors is more pronounced, as sweetness is generally perceived as pleasant, contrasting with the green and fatty aromas of these compounds.

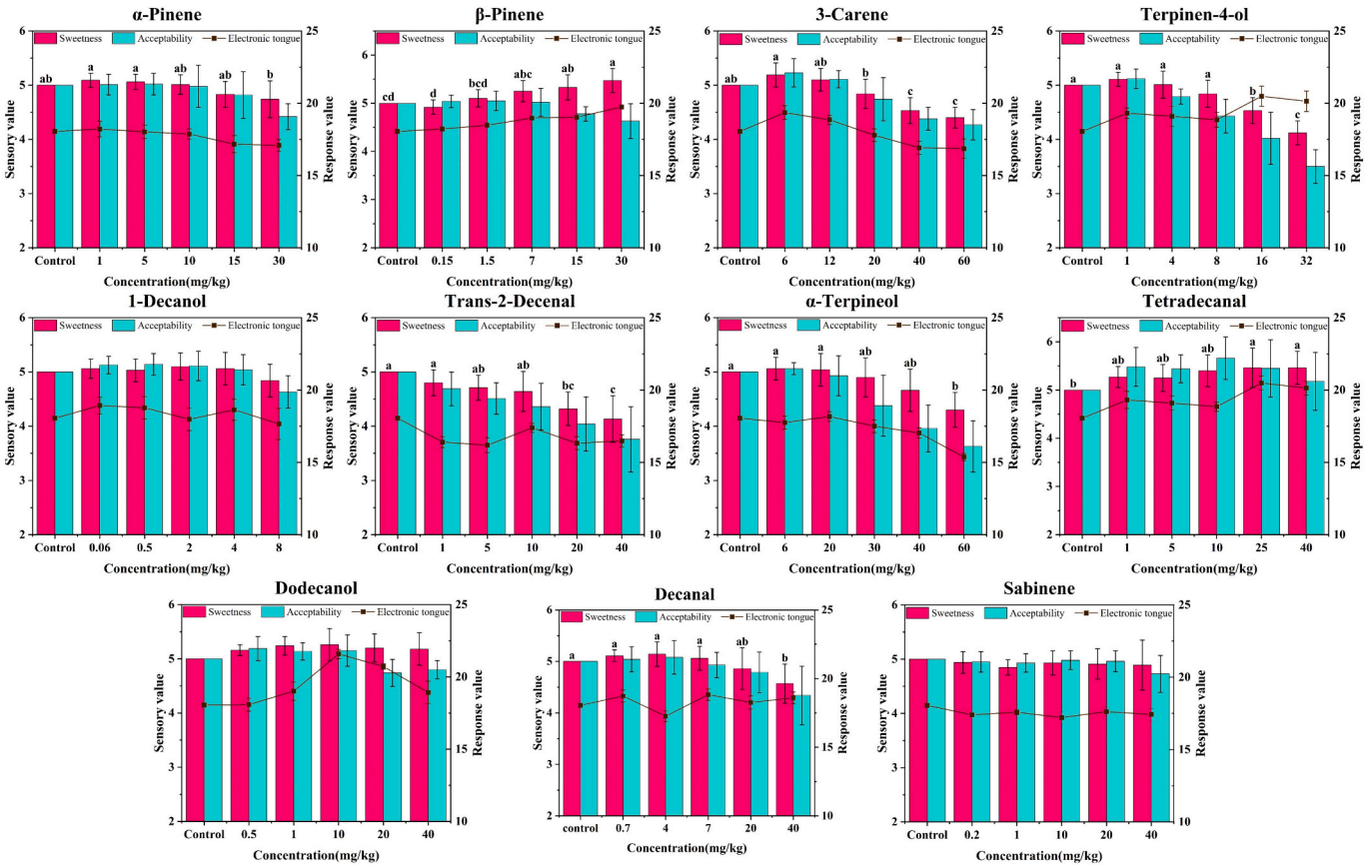

Fig. 2. The interaction diagram of 11 kinds of green and aldehyde with 5 % sucrose was presented. The error bars represented the standard error of the mean. The red bars represented sensory sweetness at each aroma concentration, the blue bars represented sensory comfort at each aroma concentration, and the brown dashed line represented the response sweetness value of the electronic tongue at each aroma concentration. (For interpretation of the references to colour in this figure legend, the reader is referred to the web version of this article.)

3.2.2. Electronic tongue

The bionic electronic tongue is capable of objectively assessing food flavor by responding to a tested sample through its taste sensors. It converts the response value into an electrical signal, which the system then processes and translates into the corresponding taste result. In this study, a 5 % sucrose solution served as the control group. Electronic tongue tests were conducted six times on the samples, yielding an average response value of 18.05. A sample with an added aroma compound was considered to have a sweetening effect if its response value exceeded 18.05. If the response value was equal to or below this threshold, the aroma compound was deemed to have no effect or an inhibitory effect on the sweetness of the sucrose solution at that concentration.

The results indicated that the sweetness response values of dodecanol, β-pinene, and tetradecanal were all higher than 18.05 at various concentrations, suggesting a certain sweetening effect of the aroma. Conversely, the sweetness response values of trans-2-decenal, α-terpineol, and terpinen-4-ol at different concentrations were all below 18.05, indicating an inhibitory effect, consistent with the findings of artificial sensory evaluation. Among these, 10 mg/kg dodecanol exhibited the highest sweetness response value (21.59), while 16 mg/kg terpinen-4-ol demonstrated the lowest sweetness response value (15.91), indicating a pronounced inhibitory effect. It is worth noting that the sweetness response value of α-pinene significantly dropped below 18.05 at higher concentrations, with the lowest response value recorded at 17.08 when the concentration reached 30 mg/kg, indicating a significant inhibitory effect. Similarly, the response value of trans-2-decenal, at any concentration, remained below 17.38, indicating a more pronounced inhibitory effect. Moreover, the sweetness response value of 1-decanol was generally high, exceeding 18.05 at concentrations ranging from 7 mg/kg to 40 mg/kg. The response values of 3-carene were relatively low at concentrations of 6 mg/kg and 12 mg/kg, while values exceeding 18.05 were observed at higher concentrations (20 mg/kg-60 mg/kg), indicating a sweetening effect, which differed from the findings of artificial sensory evaluation. This discrepancy may be attributed to the influence of sucrose, a non-volatile compound, on the release and perception of aroma substances. Additionally, pectin, as a polysaccharide present in orange juice, is also a non-volatile compound, potentially affecting the release of terpenoids and alcohols in orange juice, thus inhibiting flavor release (Li et al., 2022). Among them, 1-decanol, dodecanol, and sabinene had no significant difference between the results of artificial sense and electronic tongue. Overall, the response values of the bionic electronic tongue largely corresponded with those of artificial sensory evaluation. However, while the electronic tongue can simulate certain aspects of mammalian taste perception by converting chemical signals into electrical signals through the interaction of taste sensors and taste substances, it cannot fully elucidate the human taste mechanism. Notably, odor-induced taste enhancement (OISE) involves cross-modal perceptual interaction, with stimulation of olfactory receptors being a crucial factor, yet the electronic tongue cannot replicate this stimulation mechanism. Therefore, when using the bionic electronic tongue to evaluate the interaction between aroma and taste, discrepancies from artificial sensory results may occur.

3.3. Molecular docking

3.3.1. Taste receptor system

The Venus flytrap domain of the T1R2 subunit within the sweet taste

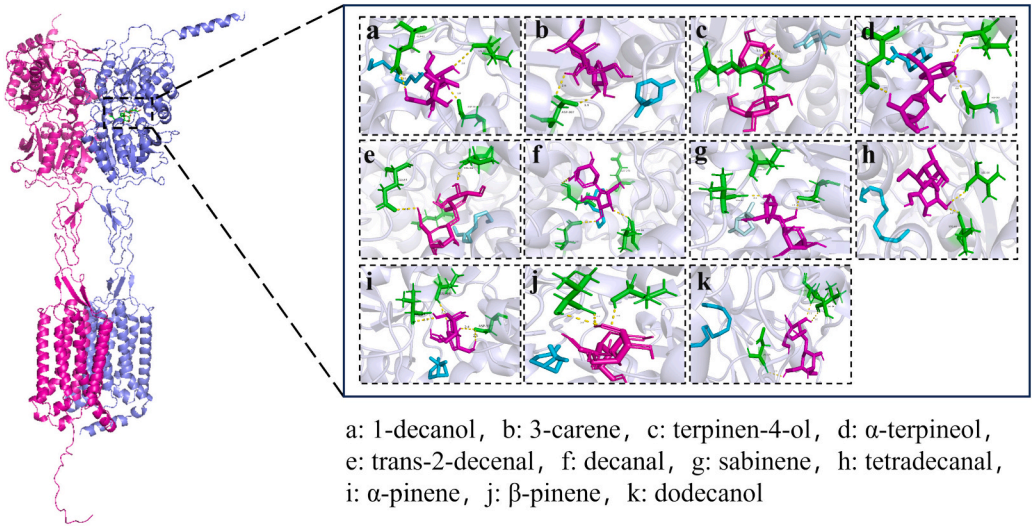

Fig. 3. Diagram of the 3D interaction between T1R2/T1R3 and sucrose, yellow dotted line represents H-bonds, blue is small molecule of green and aldehyde, and purple is sucrose. (For interpretation of the references to colour in this figure legend, the reader is referred to the web version of this article.)

receptor T1R2/T1R3 is an active site, known as the normal site, and serves as the primary structure involved in taste regulation (Mahalapbutr et al., 2019). Molecular docking in this study confirmed this, revealing that the region where sucrose molecules interact with sweet receptor proteins corresponds to the Venus flytrap domain of T1R2 (See Fig. 3). This finding aligns with the results of a study by Bassoli et al. (2014), which demonstrated that sucrose interacts with the VFD region of sweet receptor proteins through receptor cell chimera construction experiments.

To explore how various green and aldehyde compounds affect the interaction between sucrose and receptor proteins, this study created a binary complex of T1R2/T1R3 with aroma compounds. This binary complex was then combined with sucrose to form a ternary system: T1R2/T1R3-green/aldehyde compounds-sucrose. Generally, the assessment of molecular docking results' quality is often based on their binding free energy. Lower binding free energy values correspond to higher scores, with the lowest binding free energy indicative of the strongest binding mode (Servant et al., 2010; Zhang et al., 2010).

Molecular docking results for the T1R2/T1R3-green/aldehyde compounds-sucrose ternary system, including binding free energy values and interacting amino acid residues, are presented in Table 2. The binding free energy between sucrose and the receptor protein was determined to be −5.9 kcal/mol, which serves as a reference for analyzing the effects of aroma compounds on sucrose binding. Upon addition of aroma compounds, β-pinene, tetradecanal, and dodecanol exhibited binding energies of −6.1, −6.8, and − 6.3 kcal/mol, respectively. These values suggest that the presence of these substances strengthens the binding of sucrose to the receptor, leading to a sweetening effect. The key amino acid residues including VAL64, VAL66 and ASP307 are H-bonded, which occur many times, and it is speculated that they play an important role in enhancing the structural stability. By observing the hydrophobic interactions between ligands and receptors, it was found that LYS65 and LEU279 are recurring as key binding sites for aroma substances that enhance sweetness perception. The 2D figure (Fig.S3) illustrates that when β-pinene, tetradecanal, and dodecanol are introduced into the system, they interact with 5, 7, and 7 hydrophobic residues, respectively, these residues are in close proximity and facilitate the formation of a cohesive hydrophobic region. This hydrophobic environment, created by these amino acids, not only provides a suitable space for binding but also contributes to the stability of the T1R2/T1R3-sucrose complex. Conversely, the binding free energies of other aroma substances exceeded −5.9 kcal/mol, suggesting that the addition of these green and aldehyde compounds may weaken the stability of sucrose binding to sweet receptors, thereby exerting a certain inhibitory effect on sweetness. It was found that amino acid residues LEU279 and VAL309 appeared as hydrophobic residues in 9 kinds of T1R2/T1R3-green/aldehyde compounds-sucrose system, which was not expressed in T1R2/T1R3- sucrose system. These two amino acids may be the key residues of this aroma affecting the interaction of sucrose with taste receptors. Specifically, the addition of trans-2-decenal increases the binding free energy of the sucrose system to −3.4 kcal/mol, indicating that trans-2-decenal has the most significant inhibitory effect among these substances. Furthermore, the molecular docking results were in relative alignment with the outcomes of artificial sensory and electronic tongue decomposition. In this study, we demonstrated a negative correlation between the binding energy of several aroma and the ternary system of sucrose attached to the sweetness receptor proteins T1R2/T1R3 using molecular pairs and the intensity of sweetness perception. This is consistent with previous findings (Hellfritsch et al., 2012). In addition, as shown in Table 2 and Fig. S3, the binding energy does not necessarily correlate with the distance or number of hydrophobic residues. Instead, the impact of aromatic compounds on sweetness perception appears to be the outcome of the combined effects of hydrogen bonding and hydrophobic interactions. Moreover, in the ternary system, a hydrophobic interaction was established between the double ligand and the sweet taste receptor proteins T1R2/T1R3, aiding in stabilizing the closed conformation of the receptor protein VFT domain (Chéron et al., 2017).

3.3.2. *Olfactory receptor system*

Smell and taste are two primary drivers of flavor perception, influencing food flavor both independently and through transmembrane sensory interactions (Wallace, 2015). For example, odor-induced changes in taste perception (OICTP) result from these interactions between smell and taste. Shepherd (2006) demonstrated that taste perception, one of the most complex human behaviors, involves multiple senses, particularly olfactory perception. Odor images generated via the olfactory pathway contribute significantly to the formation of taste perception. In this study, two broad-spectrum olfactory receptors (OR1A1 and OR52D1) were selected for molecular docking simulations with odor substances. The results indicated that hydrophobic forces are the primary drivers of aroma substance binding to these receptors, with hydrogen bonds playing a supportive role. As detailed in Table 3, only a few ligands, such as terpinen-4-ol and 1-decanol, formed hydrogen bonds with OR1A1 at specific amino acid residues. In contrast, six ligand (terpinen-4-ol, 1-decanol, trans-2-decenal, tetradecanal, dodecanol and

Table 2
Binding energy, interaction force and key residues of sucrose, aroma and T1R2/T1R3 system.

Assembly	Binding energy (KCAL/MOL)	H-bonding of key amino acids	Hydrophobic residues
T1R2/T1R3-sucrose	−5.9	SER165、ASP142、GLU302、LYS65、ASP278、SER303	ALA166、ASN143、TYR215、TYR103、ILE306、ILE67、TRP304
T1R2/T1R3-α-pinene -sucrose	−5.3	ASP307、VAL66、VAL64	ASP278、LEU279、VAL309、GLU63、LYS65、PHE373
T1R2/T1R3-β-pinene -sucrose	−6.1	VAL64、VAL66、ASP307	PHE373、GLU63、VAL309、LYS65、LEU279
T1R2/T1R3–3-carene -sucrose	−5.6	ASP278、ASP307	GLU63、VAL64、MET45、LEU279、LEU310、LYS65、VAL309
T1R2/T1R3-terpinen-4-ol-sucrose	−4.3	ASN312、TRP455、HIS311、ARG457	THR375、ILE376、THR314
T1R2/T1R3–1-decanol -sucrose	−5.6	ASP307、ASP278、GLU63	LEU279、VAL309、VAL64、MET45、LYS65
T1R2/T1R3-trans-2-decenal -sucrose	−3.4	ASP142、SRE303、ILE306、ARG383、GLU302、LYS65	LEU71、ILE67、LIG1、VAL384、PRO308、LEU377、ASN70、VAL385
T1R2/T1R3-α terpineol -sucrose	−4.2	ASP307、VAL64、VAL66、ASP278、GLU63	ILE67、LYS65、LEU279、VAL309、ALA43、TYR282、MET45
T1R2/T1R3-tetradecanal -sucrose	−6.8	ASP307、VAL64、VAL66、ASP278、GLU63	ILE67、LYS65、LEU279、ALA43、VAL309、MET45、TRY282
T1R2/T1R3-dodecanol -sucrose	−6.3	GLU63、VAL64、VAL66、ASP307、ASP278、	MET45、TYR282、LEU279、VAL309、ALA43、LYS65、ILE67
T1R2/T1R3-decanal -sucrose	−4.8	ASP307、ILE67、VAL66、GLU63、LEU279	VAL64、ASP278、ALA43、VAL309、LYS65、MET45、TYR282
T1R2/T1R3-sabinene -sucrose	−5.2	ASP307、VAL64、ASP278、VAL66、GLU63、	LEU279、LYS65、VAL309、ALA43、MET45、TYR282

Table 3
Binding energy, interaction force and key residues of aroma and OR1A1 or OR52D1 system.

Ligand	Protein	Binding energy (KCAL/MOL)	H-bonding of key amino acids	Hydrophobic residues
α-pinene	OR1A1	−4.7		Gly232、Ile126、Val224、Ala236、Lys235、Thr239
	OR52D1	−4.2		Ala240、Ala236、Leu231、Ala128、Ile129
β-pinene	OR1A1	−4.9		Val227、Gly232、Val224、Ile126
	OR52D1	−4.1		Lys239、Thr243、Ala240、Ala128、Ile129
3-carene	OR1A1	−5.0		Val224、Ile126、Gly232、Lys235、Ala236
	OR52D1	−4.3		Ala236、Leu231、Ala240、Ile129、Ala128、Lys239
terpinen-4-ol	OR1A1	−5.1	Ser242、Thr239、Arg122	Ile287、Arg291、Tyr288、Asn292、Met59
	OR52D1	−4.2	Thr300	Lys301、Met62、Tyr296、Arg125、Thr243、Ser246、Arg299
1-decanol	OR1A1	−4.1	Val227、Val224、Ser229	Ala236、Lys235、Thr239、Ile126、Gly232、Val233
	OR52D1	−3.5	Arg299	His247、Ser246、Met62、Thr300、Tyr296、Arg125、Thr243、Ser242
trans-2-decenal	OR1A1	−3.9		Ala236、Ile126、Ser229、Gly232、Val224、Val227、Thr223
	OR52D1	−3.2	Tyr296	Met62、His247、Arg125、Thr243、Thr300、Arg299、Ser246
α-terpineol	OR1A1	−5.0	Arg122	Thr239、Met59、Ser238、Ser242、Asn292、Tyr288、Ile287、Arg291
	OR52D1	−4.5		Arg299、Thr300、Ser246、Tyr296、Arg125、Met62、Thr243
tetradecanal	OR1A1	−4.3		Ala125、Thr239、Ala236、Lys235、Gly232、Val227、Val224、Arg122、Ile126
	OR52D1	−3.3	Lys239	Ala236、Leu231、Ala128、Thr243、Ile129、Ala240
dodecanol	OR1A1	−4.0	Gly232	Lys235、Ile126、Ala125、Tyr132、Asp121、Thr239、Arg122、Ala236
	OR52D1	−3.2	Ser246、Thr243	Lys301、Glu302、Arg299、Thr300、Tyr63、Met62
decanal	OR1A1	−4.1		Gly232、Ala236、Lys235、Ile126、Ala125、Thr239、Arg122
	OR52D1	−3.7	Tyr296	Arg125、Met62、His247、Thr243、Ser246、Arg299、Ser242、Thr300

(*continued on next page*)

decanal) established hydrogen bonds with OR52D1. The binding interactions, involving numerous key amino acid residues, underscore the dominance of hydrophobic forces in aroma substance binding. The binding energy analysis revealed that the affinity of aroma compounds to OR1A1 is stronger than OR52D1, indicating a higher binding strength to OR1A1. However, this does not imply that these aroma substances do not interact with OR52D1, as the ligand specificity of olfactory receptors can be influenced by efficacy and odor characteristics (Liang et al., 2022). Molecular docking results also showed that trans-2-decenal exhibited the highest binding energy to both the T1R2/T1R3 system and olfactory receptors (OR1A1 and OR52D1), suggesting a relatively poor affinity. This could contribute to an inhibition of sucrose's sweetness perception. In addition, the binding energy of other aroma substances and key amino acids in the two systems showed no particular trend. The fact that a certain odor can enhance or inhibit the intensity of taste perception is the result of the transmembrane sensory interaction between smell and taste, involving multiple brain regions such as the olfactory bulb and the insula (De Araujo et al., 2003; Mizoguchi et al., 2016). Moreover, psychological sensory mechanisms, such as

Table 3 (*continued*)

Ligand	Protein	Binding energy (KCAL/MOL)	H-bonding of key amino acids	Hydrophobic residues
sabinene	OR1A1	−4.7		Ile126、Val227、Thr223、Val224、Val233、Gly232
	OR52D1	−4.0		Thr243、Ile129、Ala128、Ala240、Leu231、Arg125

associative learning, can also affect the perception of sweetness induced by odors (Stevenson et al., 1998), which warrants further investigation.

3.4. Molecular dynamics

In this experiment, the kinetic simulation results of T1R2/T1R3-trans-2-decenal -sucrose ternary system were analyzed to reveal the mechanism of the interaction between aroma substances and sucrose. *Trans*-2-Decenal exhibited notable inhibition of sweetness perception in artificial sensory evaluation, bionic electronic tongue analysis, and molecular docking, making it a representative example of green and aldehyde-like aromas. Therefore, trans-2-decenal was selected for MD simulation under terpolymer system to explore the binding effect of T1R2/T1R3-sucrose after the addition of aroma.

The stability of all dynamic simulation models was assessed using Root Mean Square Deviation (RMSD), the results of which are depicted in Fig. 4 (A). RMSD serves as a crucial metric and a significant indicator for evaluating the stability and reliability of simulation results. A smaller change amplitude in RMSD value over time indicates better stability during the simulation process, suggesting stable binding between the ligand and receptor. During the ligand binding process, the T1R2/T1R3-sucrose system is in a stable state after 60 ns with RMSD value of about 6.0–9.0 Å. Compared to the effect of trans-2-decenal, the binding of sucrose to T1R2/T1R3 showed significant fluctuations after 20 ns, indicating a significant conformational change in the protein structure during this simulation phase. The system remained relatively stable after 27 ns, and the RMSD value fluctuated less (approximately 7.5–9.5 Å). This indicated that the addition of the aroma affected the binding stability of T1R2/T1R3-sucrose to a certain extent, and reduced the stability of the protein. Root Mean Square Fluctuation (RMSF) was employed to characterize local changes in the protein chain. The peak value indicates the protein region with the highest fluctuations during the simulation, and the degree of atomic position fluctuation reflects the dynamic behavior of each atom in the molecule, as illustrated in Fig. 4 (B). Following the binding of sucrose ligand to T1R2/T1R3 protein, high structural flexibility was observed in the region spanning residues 800-870AA. However, with the addition of trans-2-decenaldehyde, the active region of ligand-receptor binding residues was distributed in the range of 350-360AA and 800-880AA, indicating that under the influence of aroma substances, the sweet receptor protein T1R2/T1R3 could attach fewer amino acids, thus hindering ligand-receptor binding and not promoting the stability of the ligand-receptor protein structure.

To investigate the interaction between sucrose and T1R2/T1R3, the critical amino acid residues involved in ligand binding at the T1R2/T1R3 site were further examined. Fig. 5 illustrates the fluctuation of specific amino acid interactions between ligand receptor proteins over the entire simulated trajectory process. Seven residues, namely LYS65, SER142, SER165, ASP213, ASP278, GLU302, and SER303, exhibited multiple contacts with ligands in the binary system. It was found that LSY65, ASP278 and GLU302 were the key residues involved in ligand-receptor binding during the simulation. In the ternary system under the influence of Trans-2-decenal, five crucial residues (ASN44, ASN143, SER212, ASP213, PRO241, GLN244, HIS283) were identified. This explains why the binding affinity and compactness of the T1R2/T1R3 -sucrose are higher than those of the T1R2/T1R3- trans-2-decenal -sucrose model.

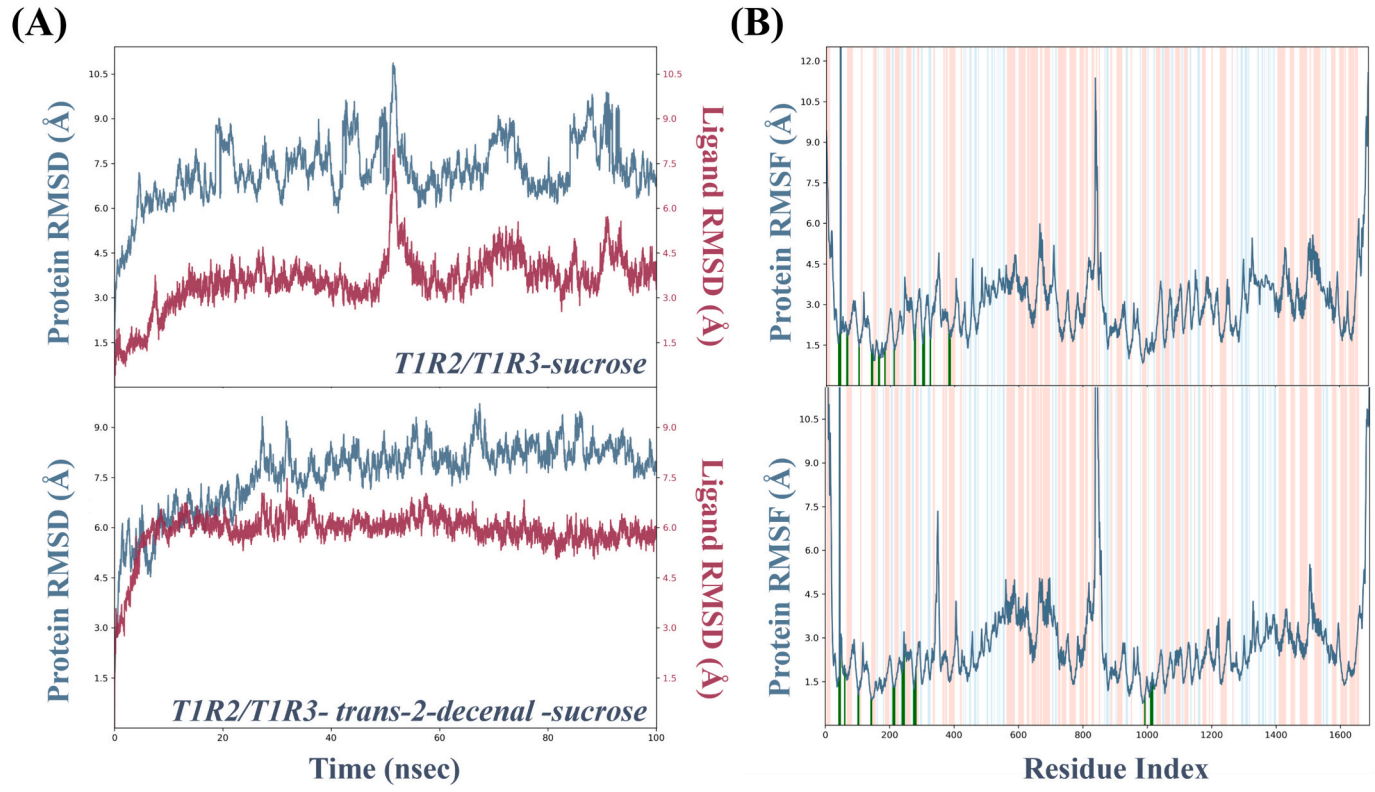

Fig. 4. (A) showed the T1R2/T1R3- sucrose complex, and the interaction between sucrose and T1T2/T1R3- trans-2-decenal complex RMSD. (B) showed the T1R2/T1R3- sucrose complex, and the interaction between sucrose and T1T2/T1R3- trans-2-decenal complex RMSF.

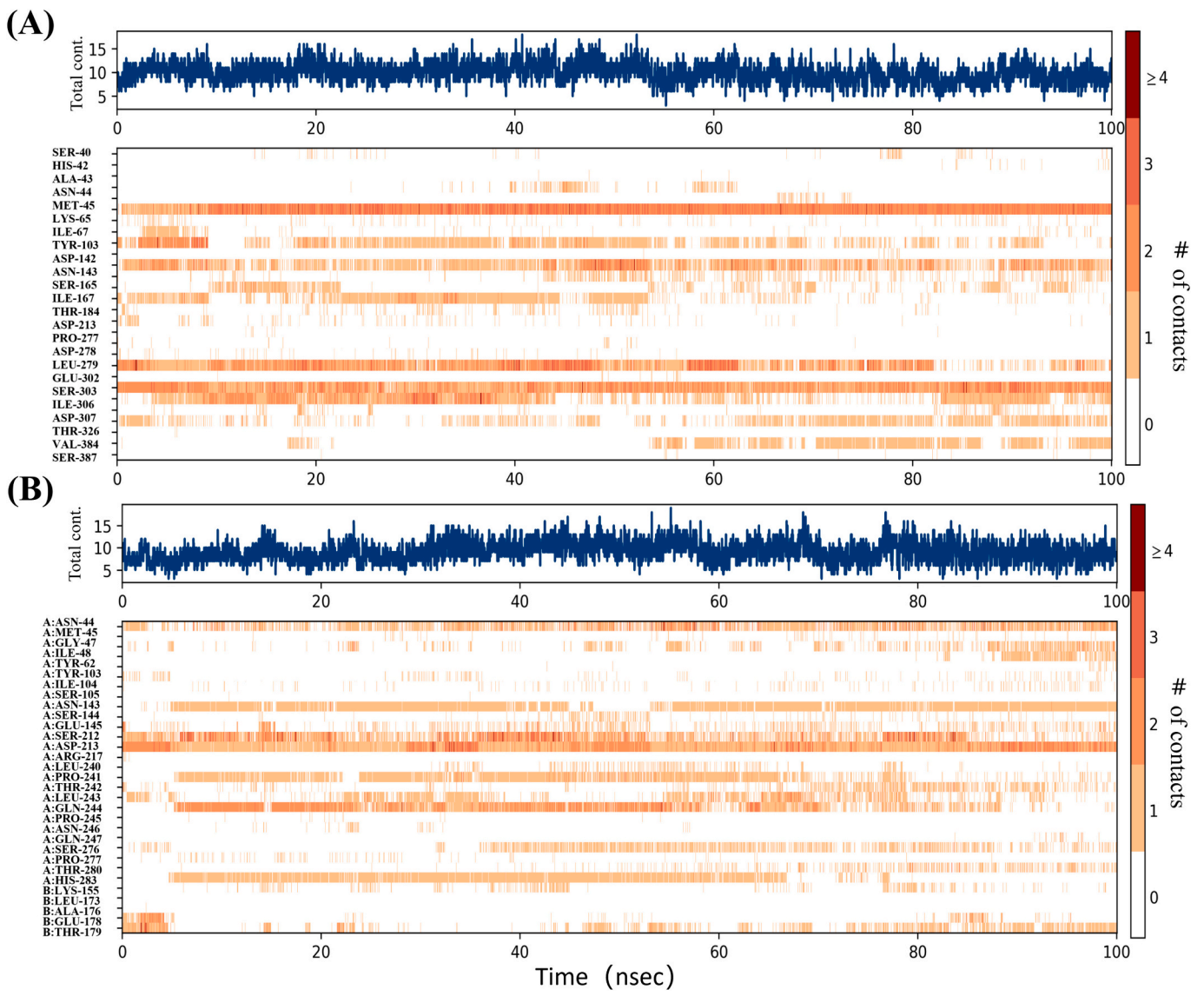

Fig. 5. (A) showed the interaction between sucrose and specific amino acids of T1R2/T1R3 protein over time, and (B) showed the interaction between specific amino acids in the T1R2/T1R3- trans-2-decenal -sucrose ternary system.

Since H-bonds is the main force inducing the formation of ligand-protein complexes, and the hot spot residues involved in sucrose ligand binding sweet receptors are polar amino acids, we further investigated the structural insights of intermolecular H-bond formation. Fig. 6 (A) showed the percentage of H-bonds in the ligand-T1R2 /T1R3 complex. It can be found that ligands in both binary and ternary systems form H-bonds with multiple polar amino acid residues in sweet receptor proteins. It is worth noting that in the interaction results where more than 30.0 % of the simulation time occurs in the selected trajectory (i.e. the interaction time exceeds 30 ns in 100 ns), Amino acid residues that form H-bonds in the T1R2/T1R3 -sucrose (12 residues: LYS65, ASP278, GLU302, SER165, SER303 directly form H-bonds; ASP142, ASP142, GLU302, VAL384, GLU303, ASP278, SER144 indirectly form H-bonds through water Bridges) more than in the T1R2/T1R3- trans-2-decenal -sucrose system (7 residues: ASP213, ASN143, GLN244, HIS283, PRO241 directly form hydrogen bonds; ASN143 and SER276 indirectly form H-bonds through water Bridges), This showed that the addition of the trans-2-decenal weakened the interaction of T1R2/T1R3 -sucrose, and thus showed inhibitory effect, which was consistent with the results of artificial sensory and bionic electronic tongue analysis. In particular, in the T1R2/T1R3- trans-2-decenal -sucrose system, ASN143 produces hydrogen bonds both directly and indirectly through water Bridges, and is the main contributing residue of ligand bonding through H-bonds, which is consistent with previous studies (Maillet et al., 2015), indicating that ASN143 is an important residue for stabilizing aspartic acid.

It is worth noting that by comparing the binding energy size of sucrose, T1R2/T1R3- green/ aldehyde -sucrose complex with the relative sweetness measured by artificial sensory experiment, we found that the trend of binding energy of the complex was consistent with the trend of experimental sweetness, as shown in Fig. 6 (B), which can be arranged in the following order: tetradecanol (−6.8 kcal/mol)>dodecanol (−6.3 kcal/mol)>β-pinene (−6.1 kcal/mol)>sucrose (−5.9 kcal/mol)>1-decanol (−5.6 kcal/mol)>3-carene (−5.6 kcal/mol)>α-pinene (−5.3 kcal/mol)>sabinene (−5.2 kcal/mol)>decanal (−4.8 kcal/mol)>terpinen-4-ol (−4.3 kcal/mol)>α-terpineol (−4.2 kcal/mol)>trans-2-decenal (−3.4 kcal/mol). Secondly, the results of kinetic simulation binding free energy analysis refer to MM-GBSA dGBind. When the value is lower than −30 kcal/mol, it indicates that the binding free energy is low and the ligand-protein binding is stable. The results of MM-GBSA in the ternary system of T1R2/T1R3- trans-2-decenal -sucrose at 0 ns, 27 ns and 100 ns are −40.72 kcal/mol, −63.63 kcal/mol and − 33.8 kcal /mol, respectively. The binding energy was lower than −30 kcal/mol in the whole

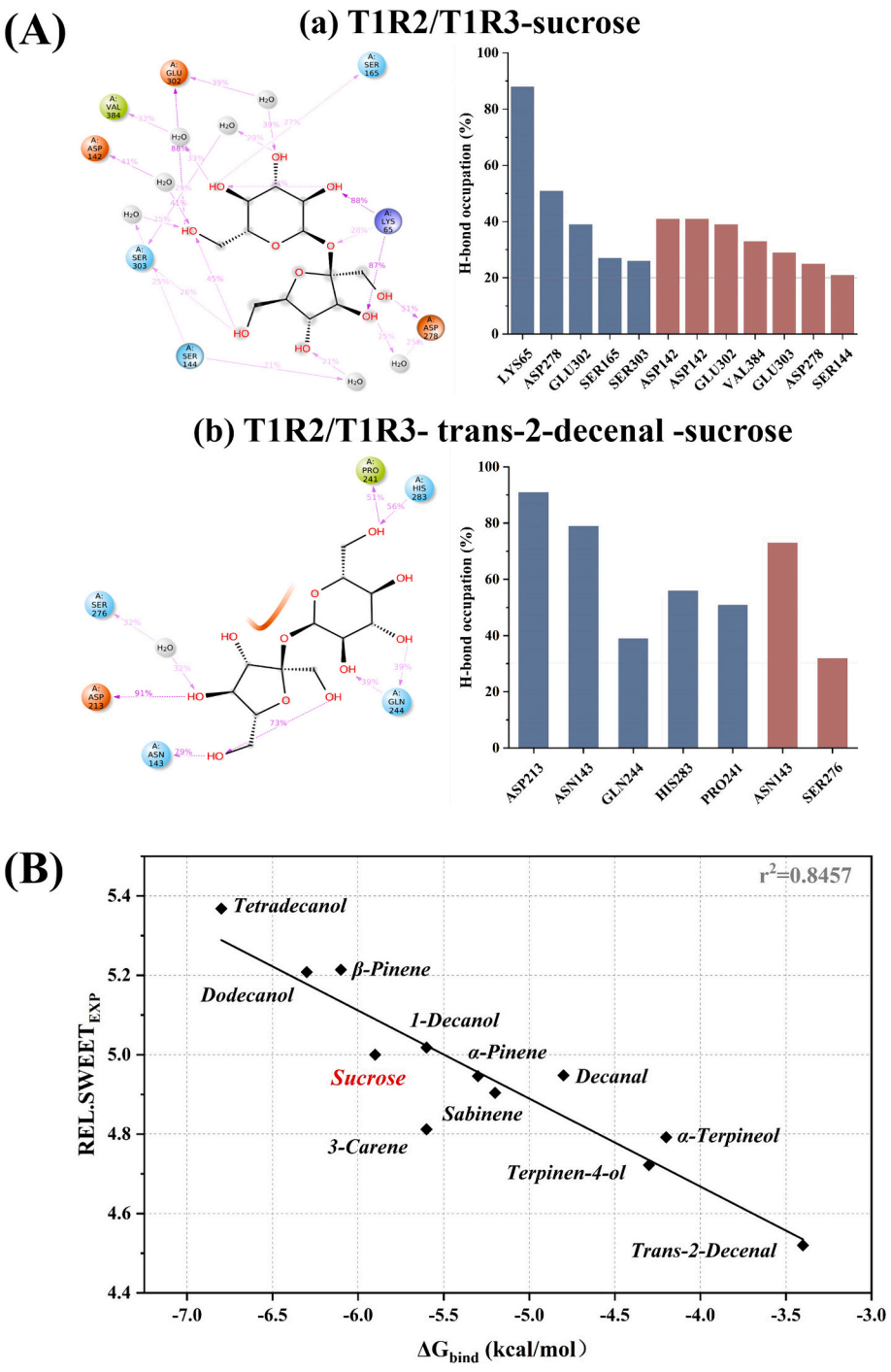

Fig. 6. (A) shows a schematic diagram of the interaction between ligand compounds and protein residues. In the binary system, interactions exceeding 30.0 % of the simulation time occur in the selected trajectory, while in the ternary system, interactions exceeding 20.0 % of the simulation time (i.e., interactions exceeding 20 ns in 100 ns) are shown. The black column represents the direct formation of H-bonds between ligands and residues, while the red represents the indirect formation of H-bonds through water bridges; (B) showed the comparison of binding free energy between relative sweetness and T1R2/T1R3- green/aldehyde -sucrose in the experiment. (For interpretation of the references to colour in this figure legend, the reader is referred to the web version of this article.)

process, indicating that the ligand-protein binding stability was good after the addition of aroma substances. At 27 ns, a short period of low binding energy appeared, which may be due to the fact that after the addition of aroma substances, sucrose molecules increased the binding competition with residues, making the ligand-protein binding ability more secure. However, with the change of time, this false firmness gradually disappeared, and at 100 ns, the MM-GBSA result increased to −33.8 kcal /mol compared with the initial, showing an inhibitory effect. In particular, compared with the simulated stable binding free energy (−32.08 kcal/mol) in the binary system, the binding free energy is lower, which may be due to the fact that the aldehyde aroma of trans-2-decenal itself does not only act on the sweet taste receptor protein, but also has a synergistic effect on other olfactory receptor proteins, which needs further study.

4. Conclusion

It is noteworthy that by comparing the binding energy of sucrose

with the T1R2/T1R3- green/ aldehyde compounds -sucrose complex to the relative sweetness measured in artificial sensory experiment, a consistent trend was observed, as depicted in Fig. 6 (B). The order of binding energy is as follows: tetradecanol (−6.8 kcal/mol)>dodecanol (−6.3 kcal/mol)>β-pinene (−6.1 kcal/mol)>sucrose (−5.9 kcal/mol)> 1-decanol (−5.6 kcal/mol)>3-carene (−5.6 kcal/mol)>α-pinene (−5.3 kcal/mol)>sabinene (−5.2 kcal/mol)>decanal (−4.8 kcal/mol)>terpinen-4-ol (−4.3 kcal/mol)>α-terpineol (−4.2 kcal/mol)>trans-2-decenal (−3.4 kcal/mol). Secondly, the kinetic simulation binding free energy analysis was performed using the MM-GBSA dGBind. A value lower than −30 kcal/mol suggests stable ligand-protein binding. The results of MM-GBSA in the ternary system of T1R2/T1R3- trans-2-decenal -sucrose at 0 ns, 27 ns and 100 ns are −40.72 kcal/mol, −63.63 kcal/mol and − 33.8 kcal /mol, respectively. The binding energy was lower than −30 kcal/mol in the whole process, indicating that the ligand-protein binding stability was good after the addition of aroma substances. At 27 ns, a short period of low binding energy appeared, which may be due to the fact that after the addition of aroma substances, sucrose molecules increased the binding competition with residues, making the ligand-protein binding ability more secure. However, with the change of time, this false firmness gradually disappeared, and at 100 ns, the MM-GBSA result increased to −33.8 kcal /mol compared with the initial, showing an inhibitory effect. In particular, compared with the simulated stable binding free energy (−32.08 kcal/mol) in the binary system, the binding free energy is lower, which may be due to the fact that the aldehyde aroma of trans-2-decenal itself does not only act on the sweet taste receptor protein, but also has a synergistic effect on other olfactory receptors, which warrants further investigation.

CRediT authorship contribution statement

ZuoBing Xiao: Funding acquisition, Formal analysis, Conceptualization. **HouWang Wang:** Writing – original draft, Investigation, Data curation. **YunWei Niu:** Writing – review & editing, Formal analysis. **JianCai Zhu:** Writing – review & editing, Formal analysis. **Yamin Yu:** Writing – review & editing, Formal analysis. **YuanBin She:** Writing – review & editing, Formal analysis. **RuJun Zhou:** Project administration, Investigation. **Zhaogai Wang:** Methodology, Formal analysis. **Jing Zhang:** Writing – review & editing, Supervision, Methodology.

Declaration of competing interest

The authors declare that they have no known competing financial interests or personal relationships that could have appeared to influence the work reported in this paper.

Data availability

Data will be made available on request.

Acknowledgement

This research was funded by the Key Projects of the National Natural Science Foundation of China (32330080). We thank the Center of Pharmaceutical Technology of Tsinghua University for the support of Desmond software and molecular dynamics.

Appendix A. Supplementary data

Supplementary data to this article can be found online at https://doi.org/10.1016/j.fochx.2024.101853.

References

Abraham, M. H., Gola, J. M., Cometto-Muñiz, J. E., & Cain, W. S. (2001). The correlation and prediction of VOC thresholds for nasal pungency, eye irritation and odour in humans. *Indoor and Built Environment, 10*(3–4), 252–257.

Acevedo, W., Ramírez-Sarmiento, C. A., & Agosin, E. (2018). Identifying the interactions between natural, non-caloric sweeteners and the human sweet receptor by molecular docking. *Food Chemistry, 264*, 164–171.

Agrawal, R., Punarva, H., Heda, G. O., Vishesh, Y., & Karunakar, P. (2023). VinaLigGen: A method to generate LigPlots and retrieval of hydrogen and hydrophobic interactions from protein-ligand complexes. *Journal of Biomolecular Structure and Dynamics*, 1–4.

Ahmed, L., Zhang, Y., Block, E., Buehl, M., Corr, M. J., Cormanich, R. A., … Ozbil, M. (2018). Molecular mechanism of activation of human musk receptors OR5AN1 and OR1A1 by (R)-muscone and diverse other musk-smelling compounds. *Proceedings of the National Academy of Sciences, 115*(17), E3950–E3958.

Ai, Y., & Han, P. (2022). Neurocognitive mechanisms of odor-induced taste enhancement: A systematic review. *International Journal of Gastronomy and Food Science, 28*, Article 100535.

Alcaire, F., Antúnez, L., Vidal, L., Giménez, A., & Ares, G. (2017). Aroma-related cross-modal interactions for sugar reduction in milk desserts: Influence on consumer perception. *Food Research International, 97*, 45–50.

Aveline, C., Thomas-Danguin, T., & Sinding, C. (2023). Ranking task versus intensity scales, what is the best method to evaluate odor-induced taste enhancement? *Journal of Sensory Studies, 38*(5), Article e12857.

Barba, C., Beno, N., Guichard, E., & Thomas-Danguin, T. (2018). Selecting odorant compounds to enhance sweet flavor perception by gas chromatography/ olfactometry-associated taste (GC/O-AT). *Food Chemistry, 257*, 172–181.

Bassoli, A., Borgonovo, G., Caremoli, F., & Mancuso, G. (2014). The taste of D-and L-amino acids: In vitro binding assays with cloned human bitter (TAS2Rs) and sweet (TAS1R2/TAS1R3) receptors. *Food Chemistry, 150*, 27–33.

Bertelsen, A. S., Mielby, L. A., Alexi, N., Byrne, D. V., & Kidmose, U. (2020). Sweetness enhancement by aromas: Measured by descriptive sensory analysis and relative to reference scaling. *Chemical Senses, 45*(4), 293–301.

Biswas, D., & Szocs, C. (2019). The smell of healthy choices: Cross-modal sensory compensation effects of ambient scent on food purchases. *Journal of Marketing Research, 56*(1), 123–141.

Boakes, R. A., & Hemberger, H. (2012). Odour-modulation of taste ratings by chefs. *Food Quality and Preference, 25*(2), 81–86.

Chéron, J.-B., Casciuc, I., Golebiowski, J., Antonczak, S., & Fiorucci, S. (2017). Sweetness prediction of natural compounds. *Food Chemistry, 221*, 1421–1425.

Ciursa, P., & Oroian, M. (2021). Voltammetric e-tongue for honey adulteration detection. *Sensors, 21*(15), 5059.

Cometto-Muñiz, J. E., & Abraham, M. H. (2008). Human olfactory detection of homologous n-alcohols measured via concentration–response functions. *Pharmacology Biochemistry and Behavior, 89*(3), 279–291.

Cometto-Muñiz, J. E., & Abraham, M. H. (2016). Dose–response functions for the olfactory, nasal trigeminal, and ocular trigeminal detectability of airborne chemicals by humans. *Chemical Senses, 41*(1), 3–14.

Dai, Y., Liu, Y., Sun, B., Yang, S., & Tian, H. (2018). Enantioselective syntheses and sensory properties of 2-Alken-4-olides. *Flavour and Fragrance Journal, 33*(2), 166–172.

De Araujo, I. E., Rolls, E. T., Kringelbach, M. L., McGlone, F., & Phillips, N. (2003). Taste-olfactory convergence, and the representation of the pleasantness of flavour, in the human brain. *European Journal of Neuroscience, 18*(7), 2059–2068.

Gemert, L.v. (2003). *Compilations of odour threshold values in air, water and other media. Second enlarged and revised ed. Beijing, China*.

Guo, Q., Liu, K., Deng, W., Zhong, B., Yang, W., & Chun, J. (2018). Chemical composition and antimicrobial activity of Gannan navel orange (Citrus sinensis Osbeck cv. Newhall) peel essential oils. *Food Science & Nutrition, 6*(6), 1431–1437.

Han, P., & Hummel, T. (2019). Orthonasal and retronasal olfaction. In *Food aroma evolution* (pp. 99–120). CRC Press.

Hellfritsch, C., Brockhoff, A., Stähler, F., Meyerhof, W., & Hofmann, T. (2012). Human psychometric and taste receptor responses to steviol glycosides. *Journal of Agricultural and Food Chemistry, 60*(27), 6782–6793.

Jiménez, J., Doerr, S., Martínez-Rosell, G., Rose, A. S., & De Fabritiis, G. (2017). DeepSite: Protein-binding site predictor using 3D-convolutional neural networks. *Bioinformatics, 33*(19), 3036–3042.

Kakutani, Y., Narumi, T., Kobayakawa, T., Kawai, T., Kusakabe, Y., Kunieda, S., & Wada, Y. (2017). Taste of breath: The temporal order of taste and smell synchronized with breathing as a determinant for taste and olfactory integration. *Scientific Reports, 7*(1), 8922.

Li, M., Zhang, W., Zhang, M., Yin, Y., Liu, Z., Hu, X., & Yi, J. (2022). Effect of centrifugal pre-treatment on flavor change of cloudy orange juice: Interaction between pectin and aroma release. *Food Chemistry, 374*, Article 131705.

Liang, L., Duan, W., Zhang, J., Huang, Y., Zhang, Y., & Sun, B. (2022). Characterization and molecular docking study of taste peptides from chicken soup by sensory analysis combined with nano-LC-Q-TOF-MS/MS. *Food Chemistry, 383*, Article 132455.

Mahalapbutr, P., Darai, N., Panman, W., Opasmahakul, A., Kungwan, N., Hannongbua, S., & Rungrotmongkol, T. (2019). Atomistic mechanisms underlying the activation of the G protein-coupled sweet receptor heterodimer by sugar alcohol recognition. *Scientific Reports, 9*(1), 10205.

Maillet, E. L., Cui, M., Jiang, P., Mezei, M., Hecht, E., Quijada, J., … Max, M. (2015). Characterization of the binding site of aspartame in the human sweet taste receptor. *Chemical Senses, 40*(8), 577–586.

Malnic, B., Godfrey, P. A., & Buck, L. B. (2004). The human olfactory receptor gene family. *Proceedings of the National Academy of Sciences, 101*(8), 2584–2589.
Malnic, B., Hirono, J., Sato, T., & Buck, L. B. (1999). Combinatorial receptor codes for odors. *Cell, 96*(5), 713–723.
Miao, Y., Ni, H., Zhang, X., Zhi, F., Long, X., Yang, X., He, X., & Zhang, L. (2022). Investigating mechanism of sweetness intensity differences through dynamic analysis of sweetener–T1R2–membrane systems. *Food Chemistry, 374*, Article 131807.
Miyazawa, T., Gallagher, M., Preti, G., & Wise, P. M. (2009). Odor detection of mixtures of homologous carboxylic acids and coffee aroma compounds by humans. *Journal of Agricultural and Food Chemistry, 57*(21), 9895–9901.
Mizoguchi, N., Kobayashi, M., & Muramoto, K. (2016). Integration of olfactory and gustatory chemosignals in the insular cortex. *Journal of Oral Biosciences, 58*(3), 81–84.
Oroian, M., Paduret, S., & Ropciuc, S. (2018). Honey adulteration detection: Voltammetric e-tongue versus official methods for physicochemical parameter determination. *Journal of the Science of Food and Agriculture, 98*(11), 4304–4311.
Pan, X., Bi, S., Lao, F., & Wu, J. (2023). Factors affecting aroma compounds in orange juice and their sensory perception: A review. *Food Research International, 169*, Article 112835.
Perez-Cacho, P. R., & Rouseff, R. L. (2008). Fresh squeezed orange juice odor: A review. *Critical Reviews in Food Science and Nutrition, 48*(7), 681–695.
Precone, V., Beccari, T., Stuppia, L., Baglivo, M., Paolacci, S., Manara, E., Miggiano, G., Falsini, B., Trifirò, A., & Zanlari, A. (2019). Taste, olfactory and texture related genes and food choices: Implications on health status. *European Review for Medical and Pharmacological Sciences, 23*(3).
Romeo-Arroyo, E., Mora, M., Pazos, N., Deba-Rementeria, S., & Vázquez-Araújo, L. (2022). Effect of product properties and context on the perception of sweetness and liking: A case study with butter cookies. *Journal of Sensory Studies, 37*(3), Article e12740.
Rother, K. I., Conway, E. M., & Sylvetsky, A. C. (2018). How non-nutritive sweeteners influence hormones and health. *Trends in Endocrinology and Metabolism, 29*(7), 455–467.
Roy, S., Narang, B. K., Gupta, M. K., Abbot, V., Singh, V., & Rawal, R. K. (2018). Molecular docking studies on isocytosine analogues as xanthine oxidase inhibitors. *Drug Research, 68*(07), 395–402.
Servant, G., Tachdjian, C., Tang, X.-Q., Werner, S., Zhang, F., Li, X., Kamdar, P., Petrovic, G., Ditschun, T., & Java, A. (2010). Positive allosteric modulators of the human sweet taste receptor enhance sweet taste. *Proceedings of the National Academy of Sciences, 107*(10), 4746–4751.
Shepherd, G. M. (2006). Smell images and the flavour system in the human brain. *Nature, 444*(7117), 316–321.
Shui, M., Feng, T., Tong, Y., Zhuang, H., Lo, C., Sun, H., Chen, L., & Song, S. (2019). Characterization of key aroma compounds and construction of flavor base module of Chinese sweet oranges. *Molecules, 24*(13), 2384.
Small, D. M., Gerber, J. C., Mak, Y. E., & Hummel, T. (2005). Differential neural responses evoked by orthonasal versus retronasal odorant perception in humans. *Neuron, 47*(4), 593–605.
Stevenson, R. J., Boakes, R. A., & Prescott, J. (1998). Changes in odor sweetness resulting from implicit learning of a simultaneous odor-sweetness association: An example of learned synesthesia. *Learning and Motivation, 29*(2), 113–132.
Strazzullo, P., D'Elia, L., Kandala, N.-B., & Cappuccio, F. P. (2009). Salt intake, stroke, and cardiovascular disease: meta-analysis of prospective studies. *Bmj, 339*.
Tao, X., Huang, Y., Wang, C., Chen, F., Yang, L., Ling, L., Che, Z., & Chen, X. (2020). Recent developments in molecular docking technology applied in food science: A review. *International Journal of Food Science & Technology, 55*(1), 33–45.
Tong, T., Wang, Y., Kang, S.-G., & Huang, K. (2021). Ectopic odorant receptor responding to flavor compounds: Versatile roles in health and disease. *Pharmaceutics, 13*(8), 1314.
Vadevoo, S. M. P., Gunassekaran, G. R., Lee, C., Lee, N., Lee, J., Chae, S., … Lee, B. (2021). The macrophage odorant receptor Olfr78 mediates the lactate-induced M2 phenotype of tumor-associated macrophages. *Proceedings of the National Academy of Sciences, 118*(37), Article e2102434118.
Wallace, M. T. (2015). Multisensory perception: The building of flavor representations. *Current Biology, 25*(20), R986–R988.
Xiao, Z., Chen, H., Niu, Y., & Zhu, J. (2021). Characterization of the aroma-active compounds in banana (Musa AAA red green) and their contributions to the enhancement of sweetness perception. *Journal of Agricultural and Food Chemistry, 69*(50), 15301–15313.
Xiao, Z., He, J., Niu, Y., Xiong, J., & Zhang, J. (2023). Characterization and comparison of aroma profiles of orange pulp and peel by GC–MS/O, OAV, aroma recombination and omission tests. *European Food Research and Technology, 249*(3), 619–630.
Yousif, R. H., Wahab, H. A., Shameli, K., & Khairudin, N. B. A. (2020). Exploring the molecular interactions between Neoculin and the human sweet taste receptors through computational approaches. *Sains Malaysiana, 49*(3), 517–525.
Yuan, S., Chan, H. S., & Hu, Z. (2017). Using PyMOL as a platform for computational drug design. *Wiley Interdisciplinary Reviews: Computational Molecular Science, 7*(2), Article e1298.
Zhang, F., Klebansky, B., Fine, R. M., Liu, H., Xu, H., Servant, G., … Li, X. (2010). Molecular mechanism of the sweet taste enhancers. *Proceedings of the National Academy of Sciences, 107*(10), 4752–4757.
Zhou, Y., & Xiao, Z. (2007). *Preparation technology of edible ffavor (1st ed.). ChinaTextile&ApparelPress*.